Morphology and phase inversion of EPDM/PP blends - Effect of viscosity and elasticity

C.F. Antunes [a], M. van Duin [b], A.V. Machado [a,],

[a] Institute for Polymers and Composites/I3N, University of Minho, 4800-058 Guimarães, Portugal

[b] DSM Research, P.O. Box 18, 6160 MD Geleen, The Netherlands

Keywords:

Morphology
Phase inversion
Co-continuity
Viscosity ratio
Elasticity ratio
Composition

Abstract

This work aims to study the effect of viscosity and elasticity ratios on the morphology and phase inversion of ethylene propylene diene monomer (EPDM)/polypropylene (PP) blends. EPDM/PP blends with a wide range of viscosity ratios and compositions were prepared in a Haake batch mixer under constant processing conditions. The composition range of EPDM/PP co-continuous morphology was investigated by selective solvent extraction and scanning electron microscopy (SEM). For the viscosity ratios used (10^{-3} to 10^{2}), a substantial composition range of co-continuity morphology was found. Our results suggest that the melt viscosity and elasticity of the major phase are the main parameters that govern the co-continuity region and phase inversion. Results obtained for phase inversion compositions were also compared with those predicted by several empirical models developed to predict the phase inversion point using dynamic viscoelastic properties of blend components. A good fit of our experimental results was obtained by adjusting the general relationship of the composition as a function of the viscosity ratio and by introducing an exponent and prefactor.

Introduction

Thermoplastic vulcanisates (TPVs) are designed to combine rubber-like properties and thermoplastic processability in a single product [1,2]. Most commercial TPVs are based on a cross-linked ethylene propylene diene monomer (EPDM) phase dispersed in a polypropylene (PP) matrix. These materials are produced by selective crosslinking of EPDM during melt-mixing with PP.

Blend properties are determined by the characteristics of each component and by the morphology and phase dimensions that develop during the melt mixing process. The final blend morphology depends on the volume composition, rheological properties of individual blend components, interfacial tension and processing conditions [1].

Heterogeneous morphologies are achieved because most polymer blends are immiscible. Thus, polymer blends can be categorized into four types: matrix-dispersed particle; matrix-fibre; lamellar structures and cocontinuous structures [3]. Co-continuous structures are particularly interesting because both components can fully contribute to blend properties. The term "co-continuous" is usually applied when a completely continuous structure is achieved for both polymers. The composition range to achieve co-continuity can be narrow or wide depending on blend system characteristics and processing conditions, and the phase inversion composition or phase inversion point is located at it centre. Phase inversion is defined as the point where blend components exchange their discontinuity. The dispersed phase becomes the matrix and vice versa. Several authors [4-7] have found that phase inversion depends on the blend composition and viscosity ratio. Thus, a theoretical prediction of the phase inversion has been proposed:

$$\frac{\phi_1 PI}{\phi_2 PI} = \frac{\eta_1}{\eta_2} \tag{1}$$

where $\phi_{1,PI}$ is the volume fraction of component i at the phase inversion point and η_1 is the corresponding melt viscosity. However, substantial deviations from Eq. (1) have been noted, especially for viscosity ratios that depart from unity [8-12]. Thus, several authors [11,13,14] have modified the general relationship by introducing an exponent and/or a prefactor to obtain better fits with experimental results. A different approach, based on Tomotika's theory of filament instability concept [15] was derived by Metelkin and Blekht [16] to predict the critical volume fraction for phase inversion:

$$\phi_2, PI = [1 + F(\lambda) \times \lambda]^{-1} \tag{2}$$

where $F(\lambda) = 1 + 2.25\log(\lambda) + 1.81[\log(\lambda)]^2$ and λ is the viscosity ratio[1].

Utracki [8] suggested another approach based on the emulsion theory that could be applied to viscosity ratios departing from unity. Using the relation given by Krieger and Dougherty [17] for monodisperse hard spheres in a fluid, and assuming that the blend viscosities that result from the addition of polymer *B* to polymer *A* and vice versa are equal at the phase inversion composition, he developed Eq. (3):

$$\lambda = \left[\frac{\phi_m - \phi_1, PI}{\phi_m - \phi_1, PI}\right]^{[n]\phi_m} \tag{3}$$

where the intrinsic viscosity [η] was assumed to be 1.9 and the maximum packing volume fraction [ϕ_m] was assumed to be 0.84 for spherical domains.

Bourry and Favis [18] suggested a model based on Van Oene's theory [19,20], which considers the elasticity contribution. It predicts the phase inversion composition in terms of elasticity using the storage modulus $G_i'(\omega)$ and tan δ_i. Furthermore, this model estimates that the more elastic phase tends to encapsulate the less elastic phase at sufficiently high concentrations during mixing.

Steinmann [21] investigated the rheological properties of blends in the phase inversion region and developed the following expression to predict the phase inversion composition:

$$\frac{\phi_1 PI}{\phi_2 PI} = \frac{G_2'(\omega)}{G_2'(\omega)} \tag{4}$$

where Z characterizes the specific interfacial area and the relaxation rate of the structure and is dependent on the blend system.

Although numerous studies have been performed on co-continuous blends and phase inversion, only limited research [12,22-28] provides detailed information on these phenomena for EPDM/PP blends with and without crosslinking. Usually, morphological characteristics of non-cross-linked EPDM/PP blends have been compared to that of corresponding dynamic vulcanisates [27-30]. Romani [22], using electron microscopy, proposed a diagram for the co-continuity region of ethylene propylene rubber (EPM) and PP as a function of the viscosity ratio and composition. Specifically, EPM/PP blends can exhibit co-continuity over a wide range of compositions depending on the viscosity ratio. Recently, Bhadane [24] studied the co-continuity of EPDM/PP blends with viscosity ratios between 0.7-5 and shear stress values between 12 – 231kPa. The co-continuity region, based on solvent extraction, for the EPDM/PP blend was symmetrical relative to the 50/50 composition, but the region was not affected by changes in the viscosity ratio.

Thus, the present work aims to investigate the phase morphology of non-cross-linked EPDM/PP blends with a wide range of viscosity ratios (10^{-3} to 10^{2}) in order to get information on phase inversion for higher and lower viscosity ratios. Moreover, the influence of the viscosity and elasticity of the blend components on morphology and phase inversion composition is studied.

Experimental

Polymers

Table 1 gives the characteristic properties of the raw polymers used in this work. All polymers are designed by a code (EPDMX or PPX), where X is complex viscosity at 65rad/s. Most of the polymers used are commercially available. However, in order to achieve very low or very high viscosity ratios, it was necessary to modify some of the commercial materials. The high viscous EPDM elastomers, EPDM6414 and EPDM1648, are commercial Keltan grades (K2340A and K5531A, respectively) supplied by DSM Elastomers, B.V. The lowest viscosity rubber, EPDM3.4, is a liquid EPDM (trilene $^{(8)}$ 67) supplied by Chemtura. EPDM6414 contains 50% by weight of oil, which was removed

using acetone under reflux for several days. The EPDM53 was prepared by controlled degradation of EPDM1648 using 0.05 parts per hundred (phr) of cumyl hydroperoxide (Acros) in an intermeshing, co-rotating Leistritz LSM 30.34 twin screw extruder at a throughput of 0.33 kg/h, a screw speed of 10 rpm and a barrel set temperature of 380°C. The high viscosity PP homopolymers (PP2116, PP950, PP443 and PP184) are commercial grades (531P, 524P, 575P and 579S, respectively) supplied by Sabic Europe. The low viscosity PPs (PP48 and PP4.6) were prepared by controlled degradation of PP184 in a Haake Rheomix 600 OS internal mixer

Table 1
Properties of blend components.

Material code	MFI[a] (g/10 min)	Mw (kg/mol)	Ethylene content (%)	ENB content (%)	η^{*b} (Pa s)
EPDM6414		510	63	4.4	6414
EPDM1648		150	53	5.7	1648
EPDM53		47	56	4.0	53
EPDM3.4		7.2	46	9.5	3.4
PP2116	0.3				2116
PP950	2.0				950
PP443	10.5				443
PP184	47				184
PP48					48
PP4.6					4.6

MFI = Melt flow index; Mw = Molecular weight; ENB = Ethylidene norbornene; η^* = complex viscosity.
[a] at 230°C and 2.16 kg .
[b] at 200°C and 65rad/s (estimated average shear rate in the internal mixer). equipped with two counter-rotating rotors using Trigonox T101 (DHBP, Akzo Nobel) as initiator. The mixer was operated at a set temperature of 200°C, 80rpm for 5 min . Trigonox T101 was used at 0.01 and 0.1 phr to prepare PP48 and PP4.6, respectively. Irganox 1076 (purchased from Ciba) was used as a stabilizer.

Rheological characterisation

The rheological behaviour of PP and EPDM was characterised by dynamic rheological measurements in a stresscontrolled AR-G2 rotational rheometer (TA Instruments) using parallel-plate geometry (diameter = 25 mm; gap = 1 mm). EPDM53 and EPDM3.4 are viscous liquids at room temperature and were put directly into the rheometer. Other materials were compression-molded into discs of 25 mm diameter and 1 mm thickness at 200°C using a 30 ton press. Frequency sweep experiments were performed at 200°C in a

range of 0.1 – 100rad/s. The linear viscoelastic domain was previously determined for each polymer. Table 1 provides the complex viscosity (η^*) at 65rad/s. This value was calculated using the model developed by Bousmina [31]

Blend preparation

A series of blends with varying viscosity ratios and EPDM/PP compositions between 10/90 to 80/20 (w/w) were prepared in the internal mixer (Haake Rheomix 600 OS) by combining the EPDM and PP polymers presented in Table 1. The rotor speed was 80 rpm and the set temperature was 200°C. The mixing sequence involved introducing PP pellets into the hot mixer. After melting the PP, the stabilizer (Irganox 1076) was added (0.25 wt.% relative to the total polymer mass), and finally the EPDM rubber was incorporated. The torque reached a constant value after about 3 min , indicating that a homogenous melt had formed. Samples were collected after an additional 5 min of mixing. Samples were cooled between two metal plates to avoid morphological changes.

Solvent extraction

Solvent extractions were performed to determine the composition range where the EPDM/PP blends exhibited a droplet-in-matrix or co-continuous phase morphology. Samples were weighed and immersed in cyclohexane at room temperature for 48 h under gentle stirring. The cyclohexane was refreshed after 24 h . Samples were weighed again after drying in a vacuum oven at 100°C for 12 h with nitrogen purging. Because cyclohexane selectively extracts the EPDM phase, the co-continuity index of the EPDM phase was calculated with the following equation as the percentage of the EPDM phase that was extracted:

$$CC_{\mathrm{EPDM}} = \frac{w_i - w_f}{w_1} \times 100 \tag{5}$$

where w_i is the weight of the EPDM phase present in the original EPDM/PP blend and w_f is the weight of the EPDM phase in the sample after solvent extraction. Sample thickness was sustained between 2 – 3 mm (approximately 200 mg) because the co-continuity index depends on sample thickness [32]. The PP continuity was qualitatively classified by the visual aspect of the final solution. PP was considered fully continuous if the sample preserved its shape and did not disintegrate. The PP phase was considered to be partially dispersed if samples disintegrated into small fragments in the cyclohexane solution. The PP phase was considered fully dispersed if a milky solution was observed.

Scanning electron microscopy (SEM)

EPDM/PP blends morphology was analyzed by SEM using a Leica Scanning Electron Microscope. The samples were fractured in liquid nitrogen and then vapour-stained with ruthenium tetroxide for 120 min . SEM in the backscattering mode (BSE) was performed on samples coated with a gold thin layer. The average areas of the dispersed phase were quantified using image analysis software (Image-Pro Plus). To obtain representative results, at least 100 particles were examined.

Results and discussion

Rheological behaviour of the blend components

Dynamic rheological measurements were performed to characterize the polymers (PP and EPDM) at applied processing conditions (i.e., set temperature and shear rate). Fig. 1 represents the complex viscosity (η^*) of various EPDM and PP materials at 200°C, as a function of frequency. While high molecular weight rubbers (EPDM6414 and EPDM1648) show shear thinning behaviour over the complete range of frequencies, low molecular weight rubbers (EPDM53 and EPDM3.4) and low molecular weight PPs (PP48 and PP4.6) display a Newtonian plateau over most of the frequency range. Shear thinning behaviour is observed only at high frequencies. Other polymers show pseudo-plastic behaviour with a Newtonian plateau at lower frequencies and shear thinning behaviour at higher frequencies.

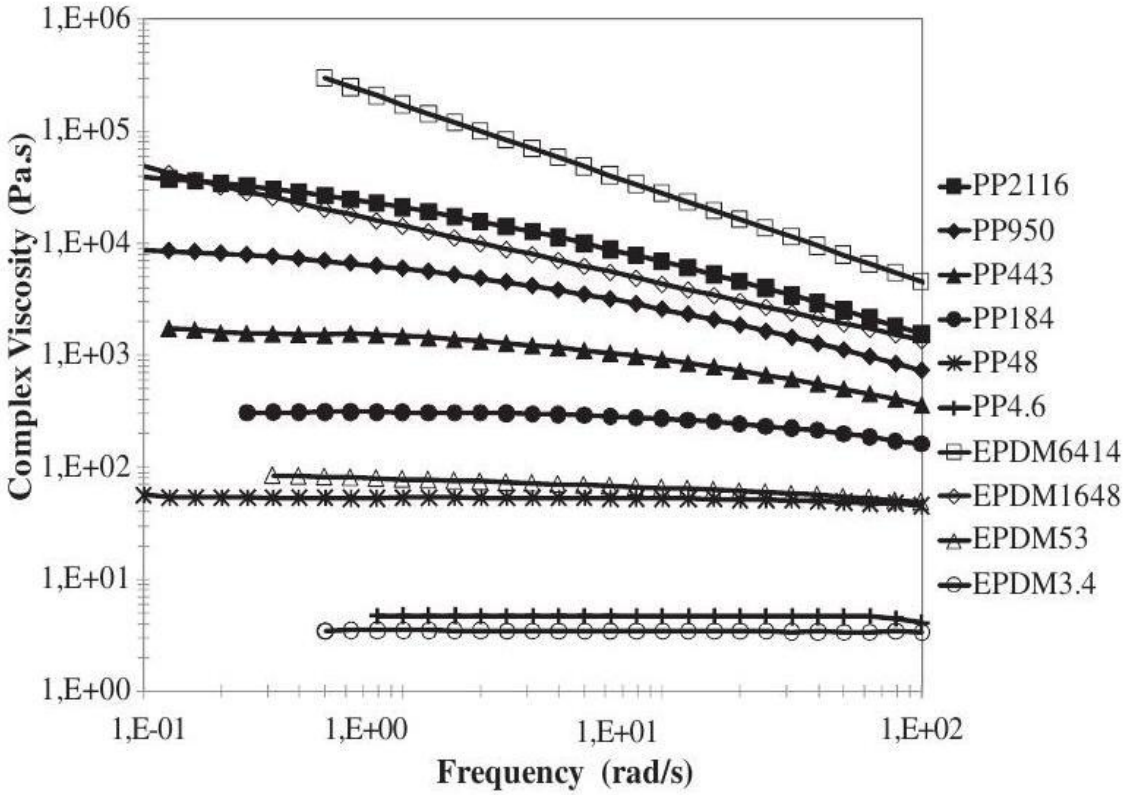

Fig. 1. Complex viscosity (η^*) of various PP and EPDM polymers at 200°C as a function of frequency.

The viscosity ratios of EPDM and PP polymers at 200°C and at an average shear rate of 65 rad.s varied five orders of magnitude (from 10^{-3} to 10^{2}) and the elasticity ratios eight orders of magnitude (from 10^{-4} to 10^{4}).

Extraction of EPDM/PP blends

EPDM co-continuity index (%) for the EPDM/PP blends are shown in Fig. 2. No quantitative data on PP co-continuity were collected because no solvents are available that can selectively dissolve PP. The structure was considered to be co-continuous if the co-

continuity index of the extracted component was 100% and the sample remained intact after extraction. The structure was fully dispersed if the co-continuity index was 0%. In most cases, values of 100% and 0% were not reached experimentally, and a relative error of $\pm$5% in the EPDM co-continuity index was determined. The EPDM was considered to be fully continuous in the blend if the corresponding co-continuity index was higher than 90%.

Fig. 2a presents the co-continuity index of blends prepared with EPDM1648. The threshold of co-continuity is nearly independent of the PP viscosity. Although all blends with 20 wt. % PP disintegrated, a milky solution was obtained only for the EPDM1648/PP4.6 blend, indicating that PP is fully dispersed in this case. For other blends of this composition, fragmentation of samples into small pieces in a milky solution was observed, suggesting that the PP is partially dispersed and partially continuous. Full cocontinuity was found in the composition range from 30 to 50wt. % PP. At 60wt. % of PP, the EPDM co-continuity index remains high (close to 90%) for most blends, suggesting that the EPDM remains continuous. The percolation point was found at 80wt. % of PP, indicating that EPDM is fully dispersed in the PP matrix. EPDM co-continuity of EPDM53/PP blends are shown in Fig. 2b. Disintegration was observed at 30wt. % of PP for all blends. However, fragmentation into small and large pieces in a milky solution was noticed for all samples, suggesting that PP was not yet fully dispersed. The lower limit of co-continuity was at 40wt. % of PP and was independent of the PP used. The higher limit of co-continuity depended slightly on the PP viscosity, being 60wt. % of PP for EPDM/PP blends prepared from higher viscosity PPs (PP2116, PP950 and PP443) and 50wt. % of PP for blends prepared with lower viscosity PPs (PP184, PP48 and PP4.3). This shift of 10wt% of PP in the upper limit of co-continuity of EPDM53 blends can be explained by the increase in the EPDM/PP viscosity ratio enhancing the tendency of EPDM to be the dispersed phase. EPDM53 is only fully dispersed at 90wt. % of PP.

Fig. 2c shows that the co-continuity interval of EPDM3.4/ PP blends depends on the PP used. The EPDM3.4/PP2100 blend disintegrated at up to 50wt. % of PP, and its cocontinuity region was between 60-80 wt.% of PP. The percolation point was observed at 90wt% of PP. For EPDM3.4/PP950 blends, fragmentation was observed at 40wt. % of PP, whereas for EPDM3.4/PP184 blends fragmentation was only observed at 30wt. % of PP. EPDM3.4/ PP184 blends display co-continuity in compositions consisting of 40-60 wt.% of PP. The co-continuity index near to the upper limit (70wt. % of PP) is higher, suggesting that the EPDM domains still have high levels of co-continuity. The shift in the lower and upper limits of the co-continuity index of EPDM3.4/PP2116 blends, when compared to EPDM3.4/

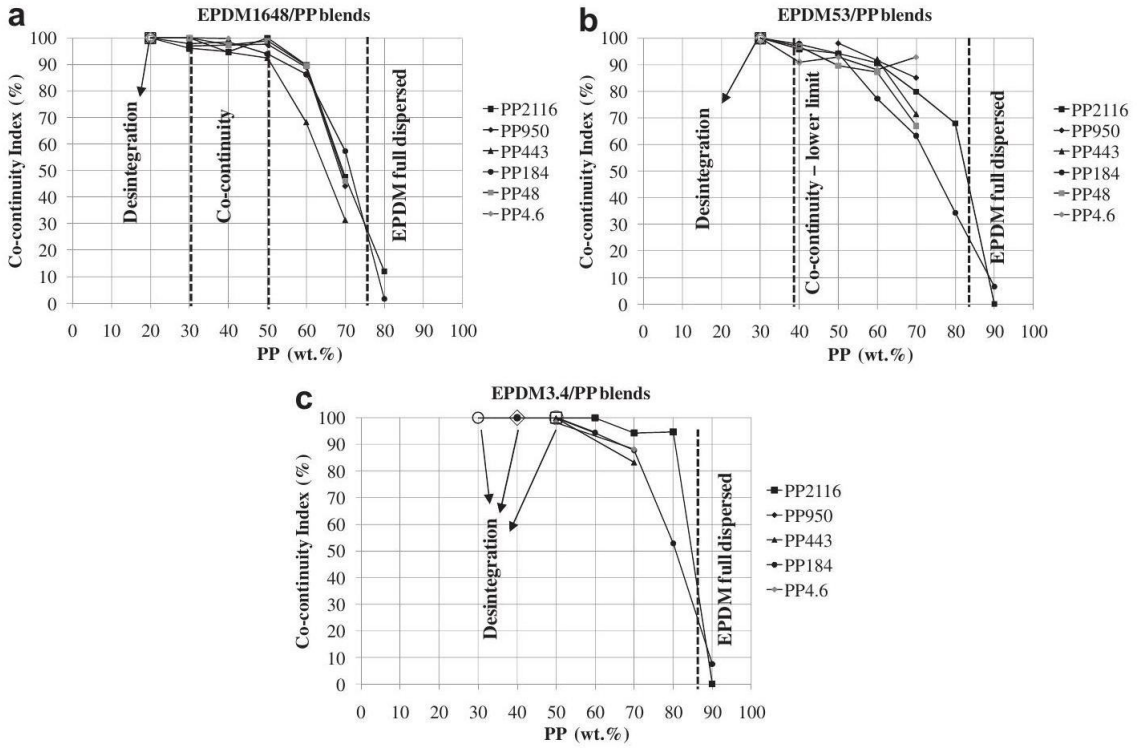

Fig. 2. EPDM co-continuity index of EPDM/PP blends as a function of the PP content (open symbols indicate disintegration of samples).

PP184 blends, was related to a decrease in the EPDM/PP viscosity ratio. EPDM3.4 blends become the matrix for PP2116 blends more readily at low PP levels because PP2116 has a much higher viscosity than PP184. At higher PP levels, the low viscosity EPDM can be substantially deformed, including the formation of elongated fibrils, which allows EPDM continuity with relatively low amounts of EPDM.

Extraction results provide evidence that the threshold of EPDM phase co-continuity depends on the viscosity of both EPDM and PP phases. For EPDM1648 blends, the EPDM co-continuity index is nearly independent of the PP type used, hence independent of the viscosity ratio. For low viscosity EPDMs, the EPDM co-continuity index depends on the PP viscosity, mainly for EPDM3.4 blends. A remarkable observation was that blends prepared with EPDM53 and EPDM3.4 and with high viscosity ratios (EPDM53/PP48, EPDM53/PP4.6 and EPDM3.4/PP4.6) did not have the same behaviour as blends prepared with EPDM1648 and similarly high viscosity ratios. This finding suggests that both viscosity and elasticity ratios probably play a role in phase morphology, which will be discussed later.

Morphology of EPDM/PP blends

Even though SEM analysis of blends made with EPDM1648, EPDM53, EPDM3.4 and EPDM6414 was performed for all prepared samples, only the results obtained for EPDM53 will be presented and discussed. The micrographs of Fig. 3 correspond to several PPs (y-axis) and different blend compositions (x-axis). The PP viscosity decreases from the bottom to the top, therefore the EPDM/PP viscosity ratio varies between 2.5×10^{-2} (PP2116) and 1.2×10^{1} (PP4.6). For well defined dispersed-matrix morphology, the area

of the dispersed domains were evaluated.

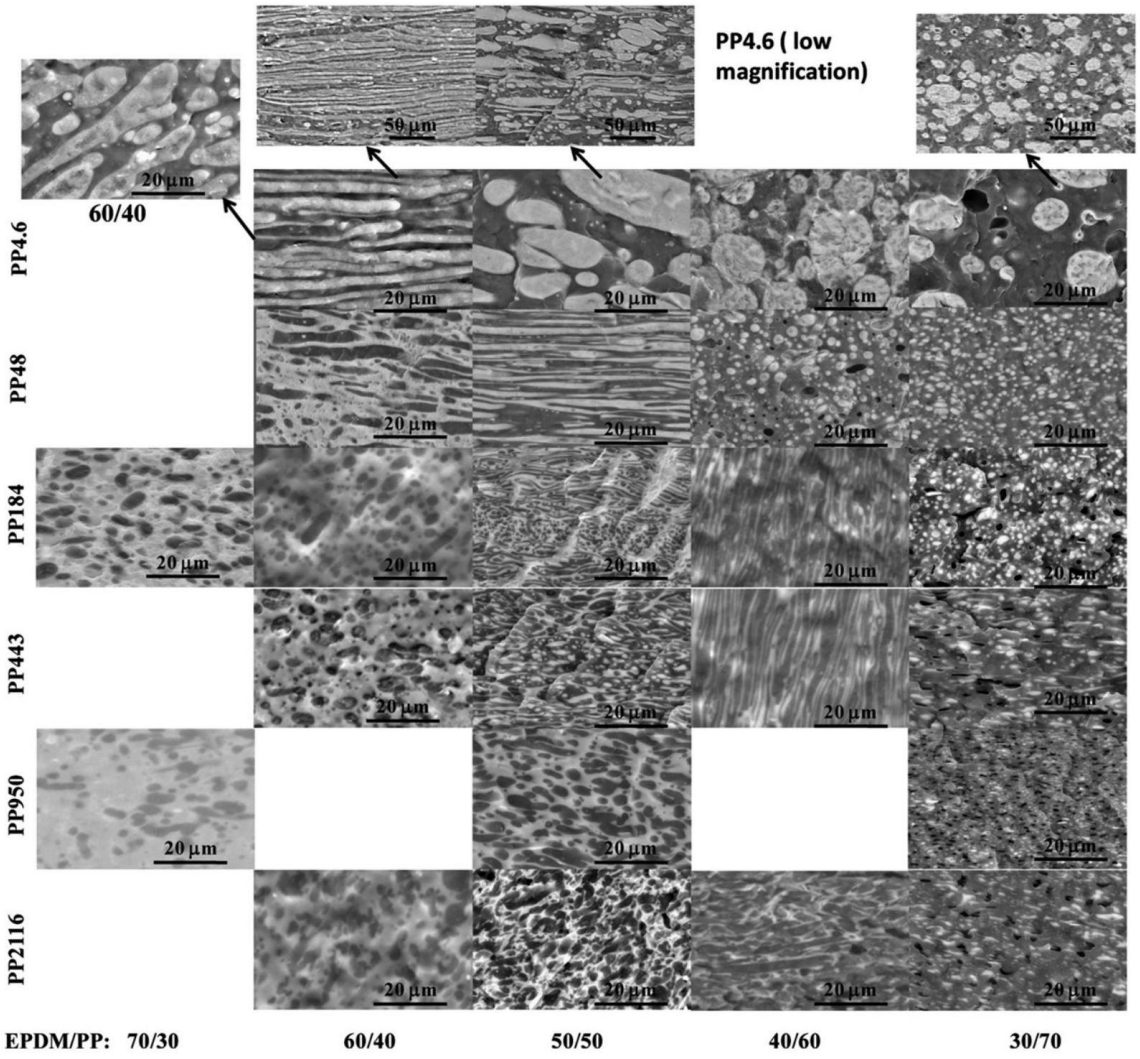

Fig. 3. SEM micrographs of EPDM53/PP blends with compositions ranging between 30 – 70wt% of PP.

SEM micrographs were only obtained for EPDM53/ PP950 and EPDM53/PP184 blends with 30 wt.% of PP because the other samples were too sticky due to the very low EPDM viscosity.

PPs seemed to be the dispersed phase for all 30 and 40wt.%PP blends with the exception of the blend containing PP4.6. PP domains of the EPDM53/PP2116 blend, which has a lower viscosity ratio, had an average area of $1.3 \times 10^{1} \mu\ \mathrm{m}^2$ in an area range of $4.9 \times 10^{-1} - 2.9 \times 10^{2} \mu\ \mathrm{m}^2$. The average area decreased to $1.0 \times 10^{1} \mu\ \mathrm{m}^2$ (range of $2.4 \times 10^{-1} - 1.8 \times 10^{2} \mu\ \mathrm{m}^2$) as the viscosity ratio increased below unity for the EPDM53/PP184 blend. An increase in the average area to $1.7 \times 10^{1} \mu\ \mathrm{m}^2$ (range of 4.2×10^{-1} $4.4 \times 10^{2} \mu\ \mathrm{m}^2$) was observed for the EPDM53/PP48 blend, which was not expected because the viscosity ratio is 1.3 . The latter results can be explained by the extraction results. The EPDM co-continuity index was around 95% and the remaining sample did not disintegrate,

indicating that PP was the continuous phase. Thus, the PP phase became the matrix as the PP viscosity decreased to levels less than the EPDM viscosity. Likewise, for blends containing PP2116 and PP184, PP domain aspect ratios were consistent with one another at about 1.5, but increased to 3 for PP48. For the EPDM53/PP4.6 blend, which had the lowest PP viscosity, the PP phase seemed to encapsulate the EPDM phase at 40wt.% of PP. EPDM co-existed as a dispersed phase and elongated structures (low magnification images). The area range of the dispersed EPDM phase varied between $5.4 - 5.5 \times 10^2 \mu\ m^2$ with an average area of $1.2 \times 10^2 \mu\ m^2$.

For PP-rich compositions at 70wt.% of PP, where most of the EPDM was dispersed, morphologies were significantly more refined than blends containing less PP at 30wt.% where PP was dispersed. The EPDM53/PP4.6 blend was an exception. EPDM domains have a relatively large area of $3.0 \times 10^2 \mu\ m^2$ (range of $4.0 \times 10^{-1} - 3.8 \times 10^3 \mu\ m^2$) because the low viscosity PP4.6 matrix cannot break up the EPDM phase. For blends with low EPDM/PP viscosity ratios, the area of the dispersed EPDM phase increased as the viscosity ratio increased. Specifically, the following average areas and area ranges were determined: $4.5 \times 10^{-1} \mu\ m^2$ ($2.0 \times 10^{-2} - 2.9 \mu\ m^2$) for the EPDM53/PP2116 blend; $9.6 \times 10^{-1} \mu\ m^2 (1.0 \times 10^{-1} - 4.7 \mu\ m^2)$ for the EPDM53/PP184 blend; and $1.0 \mu\ m^2 (1.6 \times 10^{-1} - 3.2 \mu\ m^2)$ for the EPDM53/ PP49 blend. The increase in the EPDM domain size can be explained by the decrease in the PP viscosity and elasticity. Consequently, the EPDM phase was less deformed and larger particles were obtained.

The phase inversion from dispersed PP phase to dispersed EPDM phase with increasing PP content seemed to occur at higher PP levels for EPDM53 blends containing PP2116. The EPDM phase is the matrix and PP is presented both as the dispersed and continuous phase at 40 and 50wt.% of PP. At 60wt.% of PP, both PP and EPDM phases seemed to be continuous, although EPDM was partly dispersed. At 70wt.% of PP, the PP phase was the matrix and the EPDM phase was fully dispersed. Thus, the phase inversion occurred at approximately 60wt% of PP. PP seemed to be the dispersed phase at up to 40wt.% of PP for the EPDM53/PP184 blends. At 50 wt.% of PP, both the EPDM and PP phases seemed to be continuous, although the PP phase sometimes appeared dispersed in the EPDM phase.

The PP phase is the matrix and contains elongated and somewhat interconnected EPDM particles at 60wt.% of PP. EPDM particles were dispersed in the PP matrix at 70wt.% of PP. Thus, phase inversion occurred between 50-60 wt.% of PP. For the EPDM53/PP48 blends, PP became the matrix at around 50wt.% of PP. For the EPDM53/PP4.6 blends, PP matrix formation occurred at approximately 40wt.% of PP. This shift in the phase inversion composition was related to the increased viscosity ratio. These results show that the morphology becomes coarser when low viscosity materials are used as a consequence of the low shear and elongation stresses generated. Inversely, the size of the dispersed phase is smaller if a high viscosity matrix is used.

Co-continuity region

Using the data obtained from extractions and SEM analysis, it was possible to plot the phase morphology diagrams of viscosity ratios as a function of PP content. Fig. 4a shows that the co-continuous region was influenced primarily by the EPDM. At higher PP levels and for low viscosity EPDMs, the EPDM co-continuity index depends on the viscosity ratio. For blends made with EPDM1648, the co-continuous region depends only on the EPDM/PP (w/w) composition. For EPDM53/PP blends, the upper limit of co-continuity

was slightly dependent on the viscosity ratio, which was attributable to PP being the matrix. As the viscosity and elasticity of the PP phase increased, the formation of elongated EPDM structures were enhanced, promoting the continuity of the EPDM phase. For EPDM3.4/PP blends, the co-continuous region changed with viscosity ratio, which is probably related to the large difference between the viscosity and elasticity of the EPDM and PP phases.

The EPDM53/PP48 and EPDM53/PP4.6 blends with viscosity ratios of 1.3 and 1.1×10^1, respectively, showed different behaviour from blends made with EPDM1648 but similar viscosity ratios. The lower limit of the co-continuity region was shifted to higher PP levels (about 10wt%) as is shown in Fig. 4a. Because the viscosity ratio of the blends was nearly the same, the viscosity of EPDM1648/PP, EPDM53/PP and EPDM3.4/PP blends with 30 wt. % of PP were investigated. The blend torque recorded at the end of mixing time was used as a qualitative measurement of the blend viscosity. Fig. 5 shows the blend torque as a function of the viscosity ratio. The viscosity of EPDM1648/PP blends was quite different from those blends made with EPDM53 and EPDM3.4. This suggests that the co-continuity region seems also to be an outcome of the final blend viscosity, which is driven here by the EPDM phase. The elasticity ratio measured by the storage modulus ratio was also evaluated. The elasticity ratios of EPDM53/PP4.6 and EPDM1648/ PP180 blends (viscosity ratios close to 1.0×10^1) were 2.4×10^2 and 1.5×10^1, respectively. Thus, to be the matrix, the EPDM53 constituent will have higher tendency to encapsulate the PP4.3 than the EPDM1648 relative to the PP180. This behaviour could explain why the EPDM53/PP4.6 blend disintegrated until 30wt. % of PP , whereas the EPDM1648/PP180 blend disintegration ceased after PP levels of 20wt%. These results suggest that the cocontinuity region is mainly governed by EPDM/PP composition and EPDM characteristics.

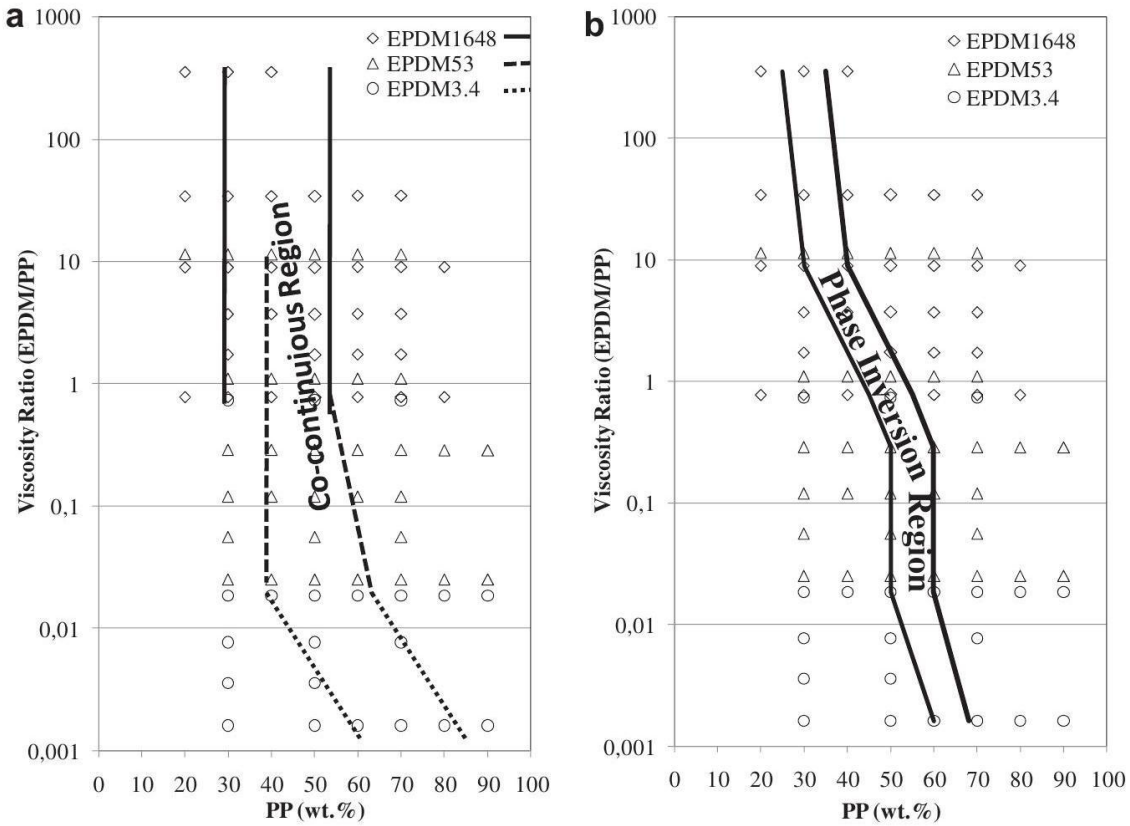

Fig. 4. Phase morphology diagram of viscosity ratios as a function of PPwt.% : a) co-continuity region and b) phase inversion region.

Another feature of these EPDM/PP blends seems to be an asymmetrical region of co-continuity at 50wt.% of PP. According to the morphology diagram suggested by Romani et al. [22], EPR/PP blends showed a relatively symmetrical region of co-continuity at 50/50 compositions and viscosity ratios of one. Moreover, a broad range of viscosity ratios around unity was noted, which becomes increasingly narrow as the viscosity ratios depart from unity. These results cannot be compared directly to the Romani diagram because their morphologies were

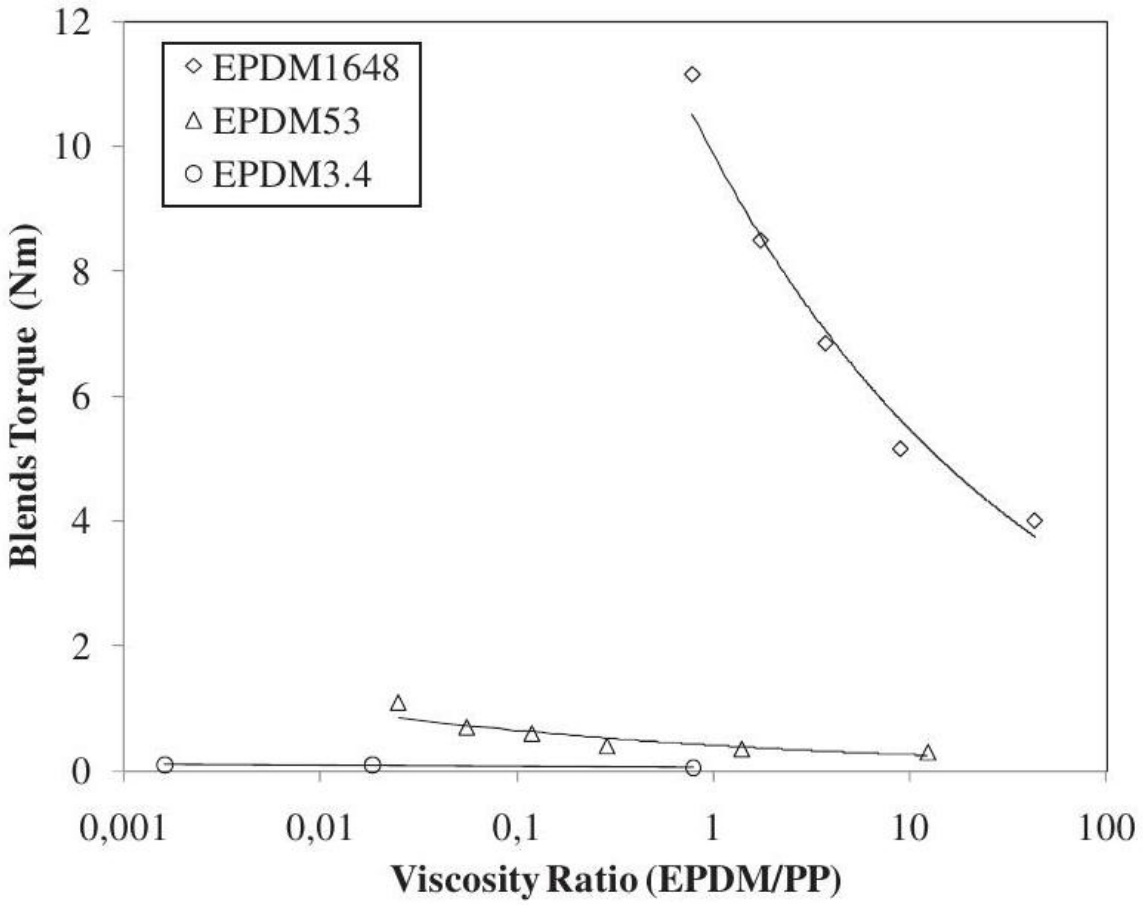

Fig. 5. End torque of 70/30 EPDM/PP blends as a function of the viscosity ratio.

obtained using SEM and Energy Dispersive X-ray Spectroscopy (EDS). Bhadane et al. [24,25] studied co-continuity based on extraction experiments (viscosity ratios ranging from $1.1 \times 10^{1} - 1.7 \times 10^{1}$). They observed asymmetrical behaviour in EPDM/PP blends and a broad co-continuity range between 35-70 wt.% of PP [26]. In another study [24], the same authors found that EPDM/PP blends (viscosity ratio between $7.0 \times 10^{-1} - 5.0$) exhibited cocontinuity ranges between $40 - 60$wt.% of PP. For high EPDM viscosity phases, a conceptual model of a collision-coalescence-separation type of erosion mechanism was proposed to explain the broadening of the co-continuity region at high viscosity ratios [25]. In the present study, although a relatively large co-continuity region was found at high and very high viscosity ratios, a widening of the cocontinuity range at high viscosity ratios (1.1×10^{1} and 1.7×10^{1}) was not observed. Differences in our results may be attributable to differences in experimental conditions (i.e., blend preparation and extraction methodology); therefore, co-continuity ranges cannot be compared.

The co-continuity region obtained from SEM-BSE microscopy (Fig. 4b) is quite narrow when compared to that obtained by extraction (Fig. 4a). This may be attributable to continuous structures appearing as a dispersed phase in SEM micrographs. Although extractions provide more accurate information on phase continuity, SEM was used to estimate the location of the phase inversion point because it narrows the co-continuity region.

As can be seen in Fig. 4b, the phase inversion region shifted to higher PP levels as the viscosity ratio decreased. The phase inversion region of EPDM53/PP blends, with viscosity ratios greater than 1 , was similar to that of EPDM1648/PP blends with similar viscosity ratios. The phase inversion region obtained by SEM-BSE was more sensitive to viscosity ratio than the co-continuous region obtained from extraction. At high viscosity ratios, an increase in the viscosity ratio from 1.0×10^{1} to 3.6×10^{2} caused a decrease of PP by 5wt% at phase inversion. However, when the viscosity ratio decreased from 1.0×10^{1} to 7.0×10^{-1}, an increase of 15 wt . % of PP was observed. Thus, phase inversion becomes less dependent on the EPDM/PP composition at higher viscosity ratios. At lower viscosity ratios, phase inversion composition was nearly unchanged for EPDM53/PP blends when the viscosity ratio varied from 3.0×10^{-1} to 2.5×10^{-2}. This observation was related to the increase in PP elasticity relative to EPDM53 elasticity as the viscosity ratio decreased. Consequently, the PP phase tends to encapsulate the EPDM phase, shifting the phase inversion region to lower PP levels and creating asymmetry relative to blends of 50/50 composition and viscosity ratios of one.

EPDM3.4/PP blends with viscosity ratio declining from 1.8×10^{-2} to 1.6×10^{-3} showed increased PP levels of 10wt. % at the phase inversion region. This decline was probably related to the low viscosity of the EPDM3.4 constituent, which tends to be matrix even at relatively high PP amounts.

Phase inversion

EPDM6614/PP blends were not included in our studies of co-continuity due to difficulties in extracting the high molecular weight EPDM rubber in cyclohexane at room temperatures. However, SEM data for these blends will be included in this section.

Influence of the viscosity ratio

To evaluate the influence of the viscosity ratio on phase inversion, experimental results will be compared to theoretical predictions using phase inversion models presented in the introduction. The phase inversion composition was estimated from morphological studies with an error of ± 5wt. % because blends were prepared in 10wt. % intervals and weight fractions were converted to volume fractions (vol.%). The experimental data describing phase inversion compositions were fitted using theoretical models of phase inversion. Results are shown in Fig. 6 as a plot of the viscosity ratio as a function of vol.% of PP. Because deviations were noted using existing models, a new expression (Eq. (6)) was developed after modification of Eq. (1) by adding an exponent and a pre-factor. Thus, at viscosity ratios of one, this outcome provides evidence that the PP 1 level is 43.4 vol . % (or 45wt. %) ($\phi_{\mathrm{EPDM}}/\phi_{\mathrm{PP}} = 1.30$) at the phase inversion composition, depending only slightly on the viscosity ratio.

$$\frac{\phi_{\mathrm{EPDM}}}{\phi_{\mathrm{PP}}} = 1.30\left(\frac{\eta_{\mathrm{EPDM}}}{\eta_{\mathrm{PP}}}\right)^{0.13} \tag{6}$$

When our experimental data were compared with models predicted by Miles and Zurek [7] and Metelkin and Blekht [16], it was found that they overestimated the phase

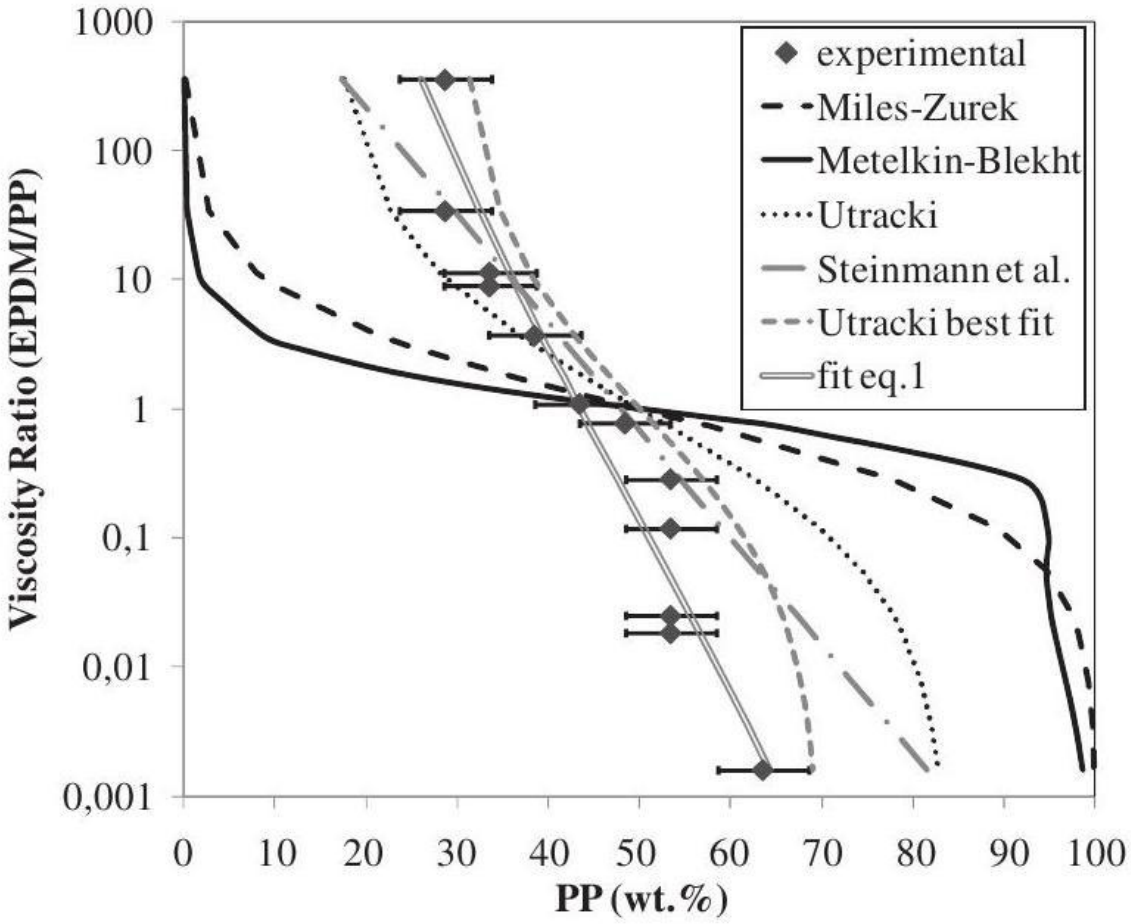

Fig. 6. Viscosity ratios of EPDM/PP as a function of vol.% PP based on theoretical predictions and experimental data.

inversion composition at viscosity ratios departing from unity. Using standard values of 1.9($[\eta]$) and 0.84(ϕ_m), the Utracki's model fits our experimental data well at viscosity ratios near and higher than one. For viscosity ratios less than one, this model overestimates the phase inversion composition. A best fit of our experimental data was obtained by changing the values of $[\eta]$ and ϕ_m to 2.5 and 0.7, respectively, although changing ϕ_m to 0.7 means that the percolation threshold is around 30vol.% of PP, which does not agree with data obtained from our extractions. The percolation threshold was close to 19vol.% of PP (20wt.%) for EPDM1648 and 9.4vol.% of PP (10wt.%) for EPDM53 and EPDM4.3. Using the ϕ_{m} experimental values, an improved fit was determined for viscosity ratios higher than one. However, the phase inversion composition was overestimated for viscosity ratios less than one. Steinman's model fits our experimental results well in viscosity ratio ranges between $1.0 \times 10^{-1} - 5.0 \times 10^{1}$.

The above discussion demonstrates that phase inversion is not a straightforward topic.

Influence of the elasticity ratio

Since for each EPDM/PP blend series, the melt elasticity increases with increasing viscosity ratio, the effect of the melt elasticity ratio could not be separated from the melt viscosity ratio. Consequently, an empirical equation similar to Eq. (6) can also be achieved using the elasticity ratio. The approach proposed by Bourry and Favis [18] was based on

the assumption that the more elastic phase has a propensity to be the matrix. It was apparent that opposite behaviour would be found by applying this model to the phase inversion composition. The same behaviour was also reported for polystyrene (PS)/polymethylmethacrylate (PMMA) blends and poly(styrene-co-acrylonitrile (PSAN)/ PMMA blends by Steinmann et al. [10]

In the present study, different EPDMs were used to obtain blends of different series at similar viscosity ratios but different elasticity ratios. For example, EPDM6414/PP184 and EPDM1648/PP48 blends have viscosity ratios around 3.5×10^1, but the elasticity ratio is 7.5×10^1 and 1.4×10^2, respectively, and the phase inversion composition was estimated to be around 20 and 30wt.% of PP, respectively. The shift may be attributable to the elasticity ratio because EPDM1647 relative to PP48 is more elastic than EPDM6414 relative to PP184. However, we did not expect a shift of 10wt% of PP with EPDM6414 as was observed when comparing EPDM6414/PP2116 and EPDM1648/PP443 blends, which have similar viscosity ratios (3.0 and 3.7, respectively) and elasticity ratios (3.3 and 4.2, respectively). Other examples are shown by the EPDM1647/PP184 and EPDM53/PP4.6 blends with viscosity ratios of 9.0 and 1.1×10^1, respectively, and elasticity ratios of 1.5×10^1 and 2.4×10^2, respectively. Although viscosity ratios for these blends are dissimilar, the variation in elasticity ratios is quite large. Thus, a shift in the phase inversion composition to higher PP levels would be expected for the EPDM53/PP4.6 blend. Nevertheless, no variation in the phase inversion composition was found (Fig. 6). These results suggest that the elasticity ratio seems not to be an effective indicator to study the influence of elasticity on the phase inversion composition. This agrees with results by Astruc et al. [33] They studied an immiscible polymer blend of polydimethylsiloxane (PDMS)/hydroxypropylcellulose (HPC) (50/50) and found that phase morphology was not influenced by elasticity ratio variations.

Conclusions

EPDM/PP blends with different viscosity ratios and compositions were prepared in a Haake batch mixer under constant processing conditions.

Solvent extraction and electron microscopy results showed that a large composition range of co-continuity morphologies for EPDM/PP blends exists under a wide range of viscosity ratios. The data suggest that the melt viscosity and elasticity of the major phases are the main parameters that drive the co-continuity region. Different cocontinuity ranges were obtained when different EPDMs and PPs with similar viscosities ratios were used. The cocontinuity region was mainly dependent on the EPDM used with the exception of blends made with low molecular weight EPDMs. Using only SEM micrographs, a narrow cocontinuity region was obtained that was used to estimate the phase inversion composition and was, therefore, determined to be the phase inversion region. The phase inversion region depended both on viscosity ratio and composition.

The experimental results for phase inversion compositions were compared with several empirical models used to predict the phase inversion point using dynamic viscoelastic properties of blend components. By introducing an exponent and a prefactor to modify the general relationship of the composition as a function of the viscosity ratio, the phase inversion composition of the EPDM/PP blends was accurately predicted for a wide range of viscosity ratios.

Acknowledgment

Authors are grateful to Portuguese Foundation of Science and Technology (PPCDT/CTM/60454/2004 and SFRH/BD/19536/2004) for the financial support.

References

[1] L.A. Utracki (Ed.), Polymer Alloys and Blends: Thermodynamics and Rheology, Hanser Publishers, Munich, 1989.
[2] D.R. Paul, in: D.R. Paul, S. Newman (Eds.), Polymer Blends, vol. 2, Academic Press, New York, 1978.
[3] P. Pötschke, D.R. Paul, J. Macromol. Sci. Part C Polym. Rev. 43 (2003) 87-141.
[4] G.N. Avgeropoulos, F.C. Weissert, P.H. Biddison, G.G.A. Böehm, Rubber Chem. Technol. 49 (1976) 93-104.
[5] D.R. Paul, J.W. Barlow, J. Macrom. Sci. Rev. Macromol. Chem. C18 (1980) 109-168.
[6] G.M. Jordhamo, J.A. Manson, L.H. Sperling, Polym. Eng. Sci. 26 (1986) 517-524.
[7] I.S. Miles, A. Zurek, Polym. Eng. Sci. 28 (1988) 796-805.
[8] L.A. Utracki, J. Rheol. 35 (1991) 1615-1637.
[9] B.D. Favis, J.P. Chalifoux, Polymer 29 (1988) 1761-1767.
[10] S. Steinmann, W. Gronski, C. Friedrich, Polymer 42 (2001) 6619-6629.
[11] V. Everaert, L. Aerts, G. Groeninckx, Polymer 40 (1999) 6627-6644.
[12] A. Valenza, G.B. Demma, D. Acierno, Polym. Net. Blends 3 (1993) 15-19.
[13] R.M. Ho, C.H. Wu, A.C. Su, Polym. Eng. Sci. 30 (1990) 511-518.
[14] N. Kitayama, H. Keskkula, D.R. Paul, Polymer 41 (2000) 8041-8052.
[15] S. Tomotika, Proc. R. Soc. Lond. A 150 (1935) 322-337.
[16] V.I. Metelkin, V.P. Blekht, Coll. J. USSR 6 (1984) 425-429.
[17] I.M. Krieger, T.J. Dougherty, J. Rheol. 3 (1959) 137-152.
[18] D. Bourry, B.D. Favis, J. Polym. Sci. Part B. Polym. Phys. 36 (1998) 1889-1899.
[19] H. Van Oene, in: D.R. Paul, S. Newman (Eds.), Polymer Blends, Academic Press, San Diego CA, 1978, pp. 295-352.
[20] H. Van Oene, J. Colloid Interface Sci. 40 (1972) 448-467.
[21] S. Steinmann, W. Gronski, C. Friedrich, Rheol. Acta 41 (2002) 77-86.
[22] D. Romanini, E. Garagnani, E. Marchetti, Int. Symp. New Polym. Mater. (1987) 56-87.
[23] S. Abdou-Sabet, R.P. Patel, Rubber Chem. Technol. 64 (1991) 769-779.
[24] P.A. Bhadane, M.F. Champagne, M.A. Huneault, F. Tofan, B.D. Favis, Polymer 47 (2006) 2760-2771.
[25] P.A. Bhadane, M.F. Champagne, M.A. Huneault, F. Tofan, B.D. Favis, J. Polym. Sci. Part B. Polym. Phys. 44 (2006) 1919-1929.
[26] F. Mighri, M. Huneault, Can. J. Chem. Eng. 80 (2002) 1028-1035.
[27] S.K. De, A.K. Bhowmick (Eds.), Thermoplastic Elastomers from Rubber-Plastic Blends, Ellis Horwood, New York, 1990.
[28] A.Y. Coran, R.P. Patel, in: G. Holden, R.K. Hans, R.P. Quirk (Eds.), Thermoplastic Elastomers, second ed. Hanser Publishers, Munich, 1996, pp. 143-181.
[29] J. Karger-Kocsis, in: G.O. Shonaike, G.P. Simon (Eds.), Polymer Blends and Alloys, Marcel Dekker, New York, 1999, pp. 125-153.
[30] S. Abdou-Sabet, R.C. Puydak, C.P. Rader, Rubber Chem. Technol. 69 (1996) 476-494.
[31] M. Bousmina, A. Ait-Kadi, J.B. Faisant, J. Rheo. 43 (1999) 415-433.
[32] J.A. Galloway, K.J. Koester, B.J. Paasch, C.W. Macosko, Polymer 45 (2004) 423-428.
[33] M. Astruc, P. Navard, Macromol. Symp. 149 (2000) 81-86.